Supporting Information

Direct observation of Mg^{2+} complexes in ionic liquid solutions by ^{31}Mg β-NMR spectroscopy

Daniel Szunyogh,[a‡] Ryan M.L. McFadden,[b,3c‡] Victoria L. Karner,[b,c‡] Aris Chatzichristos,[c,d] Thomas Day Goodacre,[e] Martin H. Dehn,[c,d] Lia Formenti,[f] Derek Fujimoto,[c,d] Alexander Gottberg,[e] Evan Kallenberg,[d] Ildikó Kálomista,[a] Rob F. Kiefl,[c,d] Flemming H. Larsen,[g] Jens Lassen,[e] C.D. Philip Levy,[e] Ruohong Li,[e] W. Andrew MacFarlane,[b,c] Iain McKenzie,[h,i] Gerald D. Morris,[h] Stavroula Pallada,[a] Matthew R. Pearson,[h] Stephan P.A. Sauer,[a] Paul Schaffer,[j] Peter W. Thulstrup,[a] Lars Hemmingsen,[a] and Monika Stachura[j]

[a.] *Department of Chemistry, University of Copenhagen, Universitetsparken 5, 2100 København Ø, Denmark.*
[b.] *Department of Chemistry, The University of British Columbia, 2360 East Mall, Vancouver, BC V6T 1Z3, Canada*
[c.] *Stewart Blusson Quantum Matter Institute, The University of British Columbia, 2355 East Mall, Vancouver, BC V6T 1Z4, Canada*
[d.] *Department of Physics and Astronomy, The University of British Columbia, 6224 Agricultural Road, Vancouver, BC V6T 1Z1, Canada*
[e.] *Accelerator Division, TRIUMF, 4004 Wesbrook Mall, Vancouver, BC V6T 2A3, Canada*
[f.] *Department of Physics, University of Guelph, 50 Stone Road E., Guelph, ON N1G 2W1, Canada*
[g.] *Department of Food Science, University of Copenhagen, Rolighedsvej 26, Frederiksberg C, Denmark*
[h.] *Physical Sciences Division, TRIUMF, 4004 Wesbrook Mall, Vancouver, BC V6T 2A3, Canada*
[i.] *Department of Chemistry, Simon Fraser University, 8888 University Drive, Burnaby, BC V5A 1S6, Canada*
[j.] *Life Sciences Division, TRIUMF, 4004 Wesbrook Mall, Vancouver, BC V6T 2A3, Canada*
[‡] *These authors contributed equally to this work*

Methods and Supplementary Results

Elemental analysis by Inductively Coupled Plasma Mass Spectrometer (ICP-MS)
Elemental purity control of the ionic liquids (EMIM-Ac and EMIM-DCA) was carried out using a Bruker Aurora Elite Inductively Coupled Plasma Mass Spectrometer. Before the ICP-MS analysis a thousand times dilution was used on both ionic liquids, with 1% ultra-pure nitric acid (Sigma-Aldrich, HNO_3, >69.9% for trace analysis). A multi element standard was used for a six-points calibration curve (Inorganic Ventures Multi-Element Standard for ICP-MS in 0-20 ppb range).

Table S1 | Concentrations of various metal ions in MilliQ water, EMIM-Ac and EMIM-DCA.

c/mM	MilliQ water	EMIM-DCA	EMIM-Ac
Mg	<3.5E-06	<3.5E-03	<3.5E-03
Ca	<1.8E-06	<1.8E-03	<1.8E-03
Fe	<3.7E-06	1.19E-00 ± 0.08E-00	<3.7E-03
Al	<9.2E-06	7.7E-01 ± 0.2E-01	4.12E-01 ± 0.11E-01
Pb	<5.9E-07	<5.9E-04	<5.9E-04
Cu	<4.8E-06	7.4E-03 ± 0.1E-01	1.48E-00 ± 0.06E-00
Ni	<2.9E-06	<2.9E-03	<2.9E-03
Cr	<2.4E-06	<2.4E-03	<2.4E-03
Mn	<2.2E-06	<2.2E-03	<2.2E-03
Zn	<2.6E-06	<2.6E-03	<2.6E-03
Co	<1.9E-07	<1.9E-04	1.22E-01 ± 0.09E-01

Properties of the ionic liquids
Table S2 | Physical properties of the ionic liquids.

	EMIM-Ac	EMIM-DCA	H_2O
Melting point (K)	228[1]	252[2]	273
Dielectric constant (T = 298 K)	–	11.0[3]	78.4[4]
Dynamic viscosity (T = 298K, mPa·s)	143.6[5]	16.1[5]	0.89[6]
Dynamic viscosity (T = 348K, mPa·s)	16.3[5]	5.3[5]	0.40[6]

NMR spectroscopy
Liquid-state NMR spectra were recorded on a Bruker Avance DRX-500 (11.7 T) spectrometer. Experiments were performed at 343.2 K (70 °C). The parameters of the various NMR measurements are presented in Table S3. Topspin 3.5 and Mestrenova 12.0 software were used to analyze the data.

Table S3 | Parameters of the NMR measurements ([1]: Using the C4-H hydrogen; [2]: using the C4 carbon as reference (methyl-group on the nitrogen of the imidazolium ring).

	^{1}H	^{13}C	^{15}N	^{17}O	^{25}Mg	^{35}Cl
Resonance frequency (MHz)	500.13	125.77	50.68	67.80	30.62	49.00
Number of scans	128	8192	2048	8192	16384*	8192
Relaxation delay (s)	5.0	2.0	2.0	0.4	1.0	0.5
Spectral width (kHz)	50	30.03	15.15	100	100	24.5
Acquisition time (s)	0.3277	0.1364	0.5407	0.1638	0.1639	0.0835
Reference	[1][7]	[2][7]	Urea in DMSO-d6	$H_2O(l)$	11 M $MgCl_2$	0.1M NaCl

*The number of scans was 131072 in experiments with 25mM $MgCl_2$ presented in the main text Figure 2. Samples for NMR spectroscopy were prepared by dissolving NaCl (anhydrous, ≥ 99.5% purity), $Mg(Ac)_2{\cdot}4H_2O$, (≥ 99.5% purity), or $MgCl_2$ (anhydrous, ≥ 98% purity) in EMIM-Ac (1-ethyl-3-methyl-imidazolium acetate purchased from Sigma–Aldrich; ≥ 95 % purity, *c*=6.033M) or in EMIM-DCA (1-ethyl-3-methyl-imidazolium dicyanamide purchased from Sigma–Aldrich; ≥98 % purity, *c*=6.264M). The sample was placed under vacuum (~$5{\cdot}10^{-3}$ mbar) overnight before the NMR experiments to reduce potential water contamination. All spectra were recorded in a double-tuned BBI probe equipped for 5 mm (o.d.) sample tubes.

Table S4 | ^{1}H NMR and ^{13}C NMR chemical shifts of the two imidazolium-based ionic liquids.

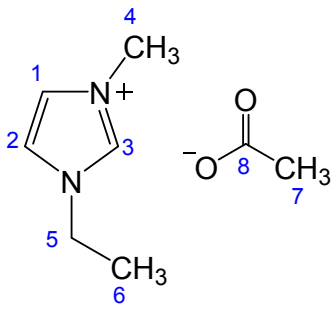

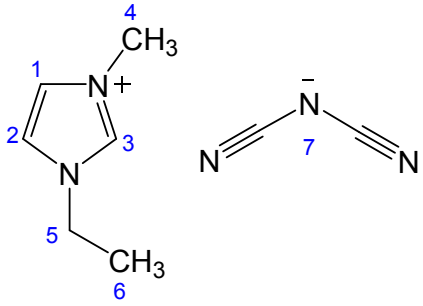

	EMIM-Ac (δ/ ppm)		EMIM-DCA (δ/ ppm)	
	^{1}H NMR	^{13}C NMR	^{1}H NMR	^{13}C NMR
1	7.86	123.81	7.23	122.71
2	8.02	122.38	7.30	121.10
3	10.16	138.28	8.58	135.60
4	3.60*	35.00*	3.60*	35.00*
5	3.90	43.78	3.93	43.98
6	0.90	14.82	1.16	13.76
7	1.12	25.14	–	118.40
8	–	174.01	–	–

*The methyl group on the imidazolium ring was used to reference the chemical shift of ^{1}H and ^{13}C[7].

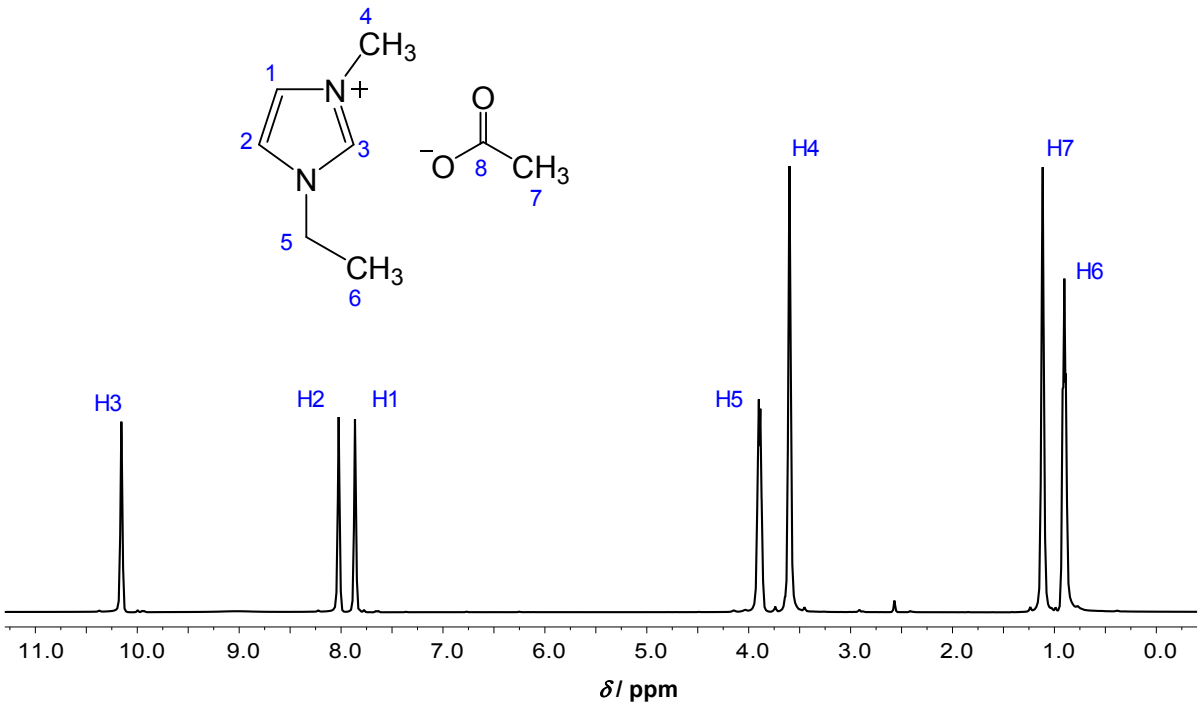

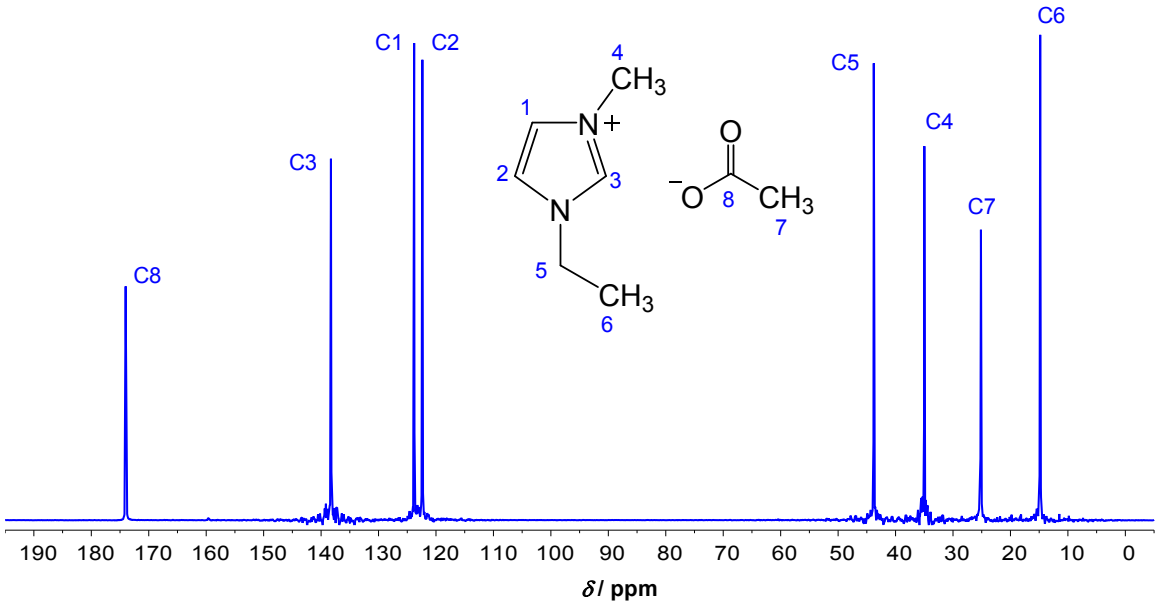

Figure S1 | ^{1}H NMR (top) and ^{13}C NMR (bottom) spectra of EMIM-Ac (T = 343 K).

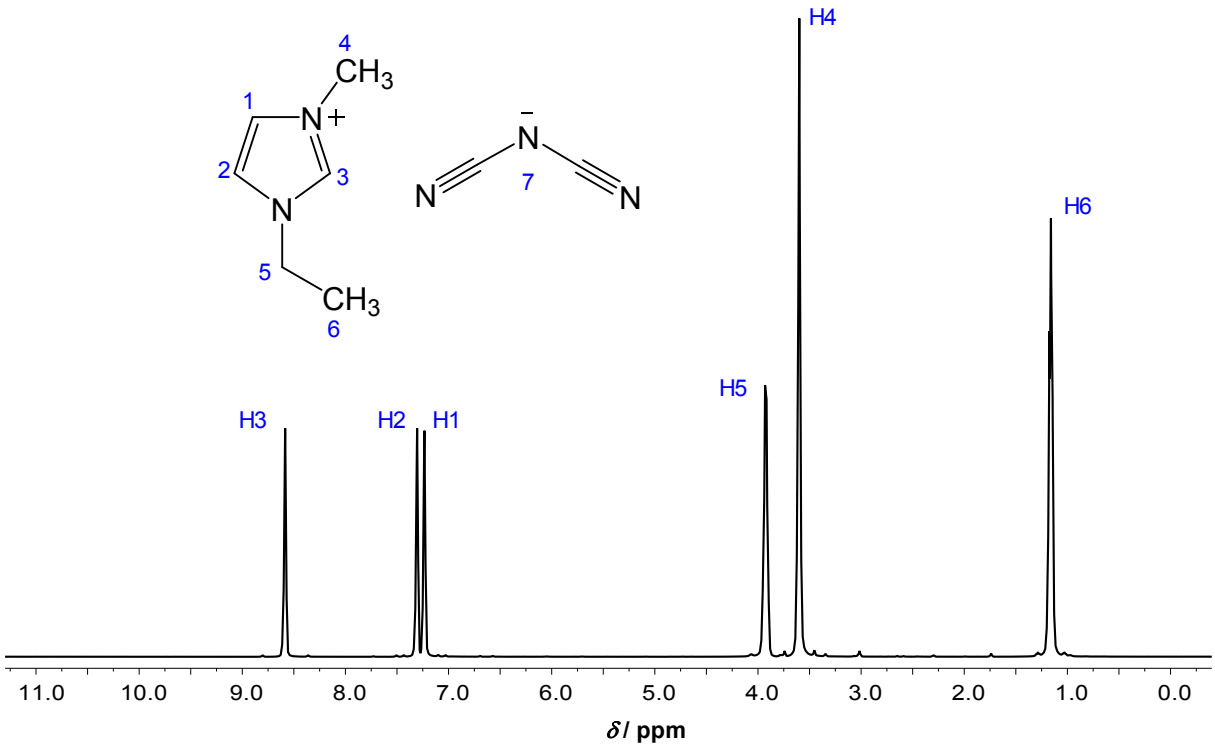

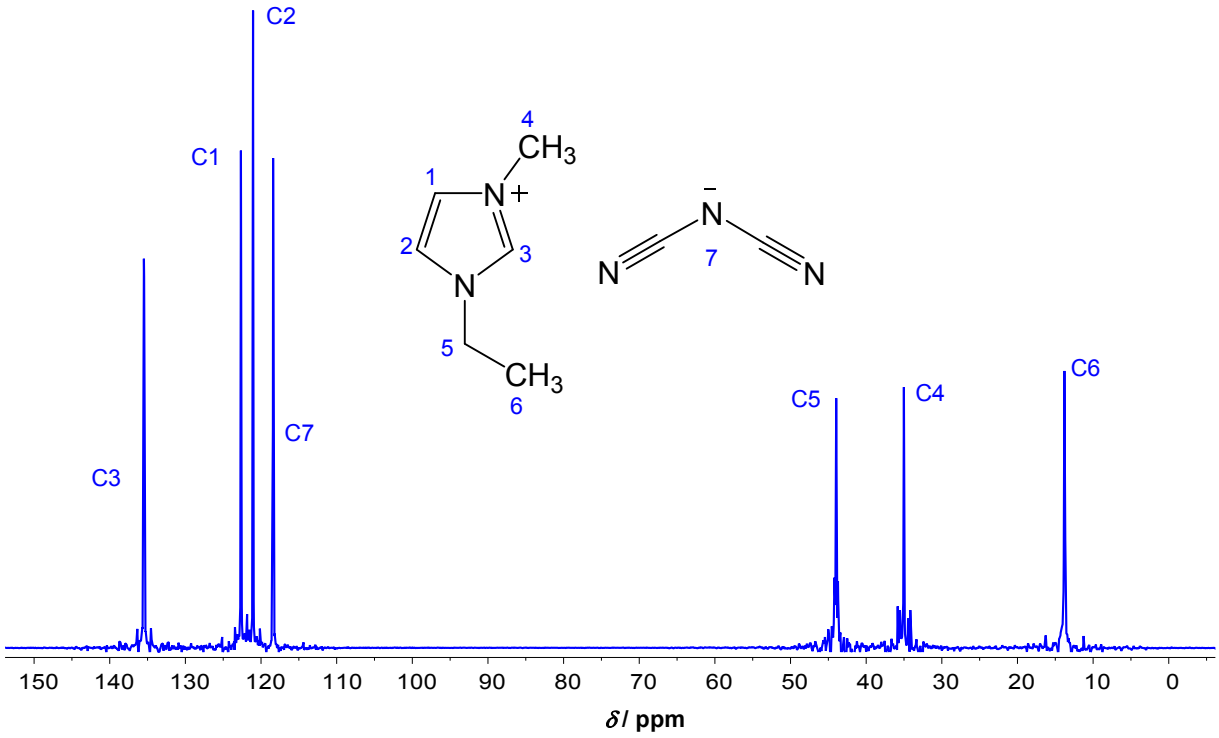

Figure S2 | ^{1}H NMR (top) and ^{13}C NMR (bottom) spectra of EMIM-DCA (T = 343 K).

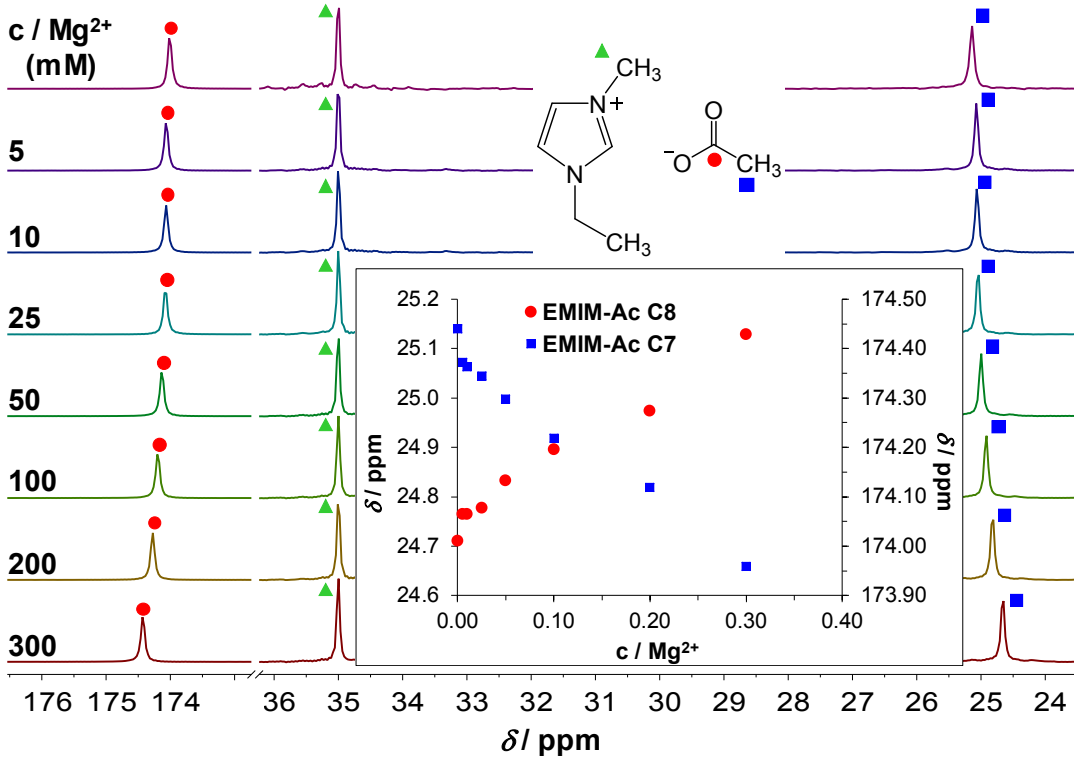

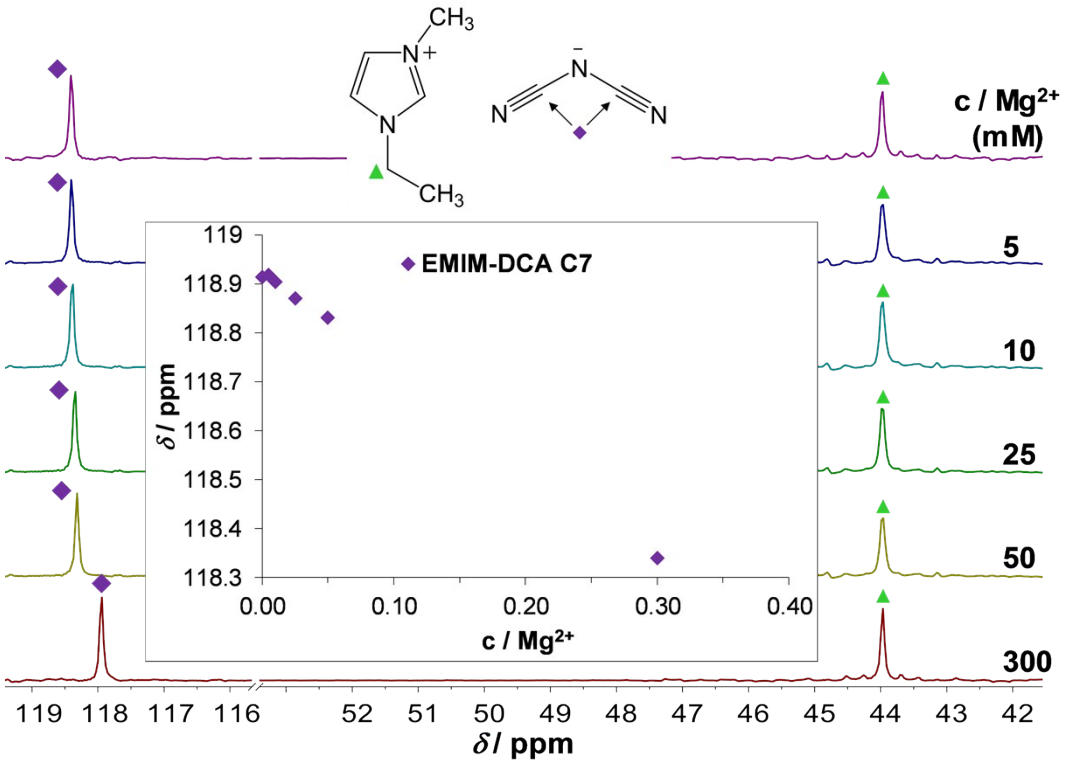

Figure S3 | ^{13}C NMR spectra of EMIM-Ac (top) and EMIM-DCA (bottom) as a function of the concentration of $MgCl_2$ (T = 343 K). The ^{13}C chemical shifts of acetate anion in EMIM-Ac are affected by addition of $MgCl_2$ (anhydrous), indicating that Mg^{2+} binds to the carboxylate oxygens as expected. The concentration of Mg^{2+} is 0-300 mM, while the concentration of acetate ion is 6.033 M. Only one narrow ^{13}C resonance is observed (for each carbon atom) in the presence of Mg^{2+}, i.e. the free and Mg^{2+} bound acetate ion are not observed individually, demonstrating that these two species are in fast exchange on the NMR time scale (ms), and similarly for the DCA anion in EMIM-DCA.

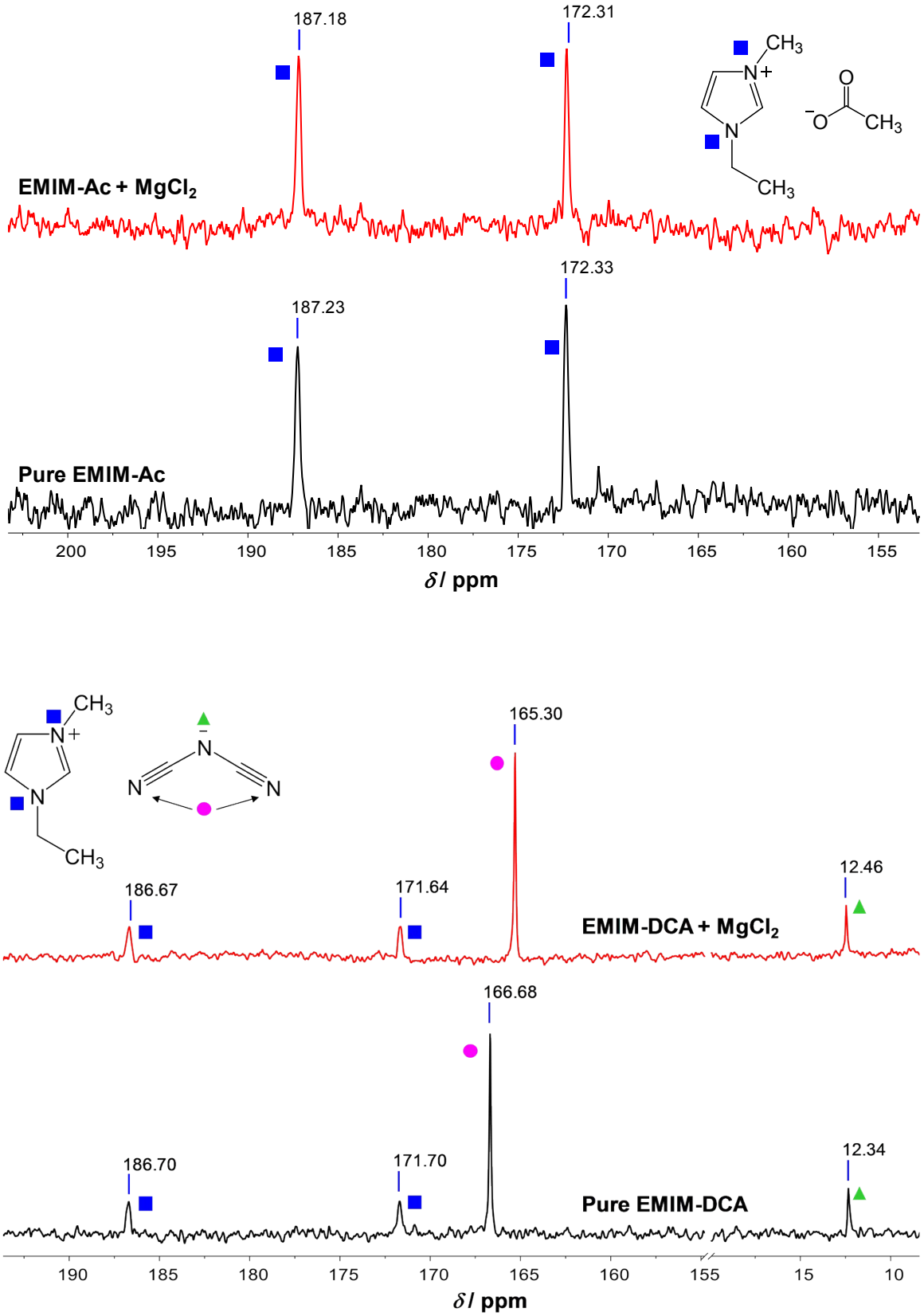

Figure S4 | Top: ^{15}N NMR spectra of EMIM-Ac with and without 300 mM $MgCl_2$; Bottom: ^{15}N NMR spectra of EMIM-DCA with and without $MgCl_2$ (T = 343 K).The chemical shifts from imidazolium nitrogen atoms as well as the central nitrogen of DCA are essentially unchanged, while a significant change is observed for the terminal nitrogen atoms of DCA, upon addition of 300 mM $MgCl_2$, indicating that the latter coordinate to Mg^{2+}. In analogy to the ^{13}C, Figure S3, the ^{15}N NMR data indicate fast exchange between free and Mg^{2+} bound DCA.

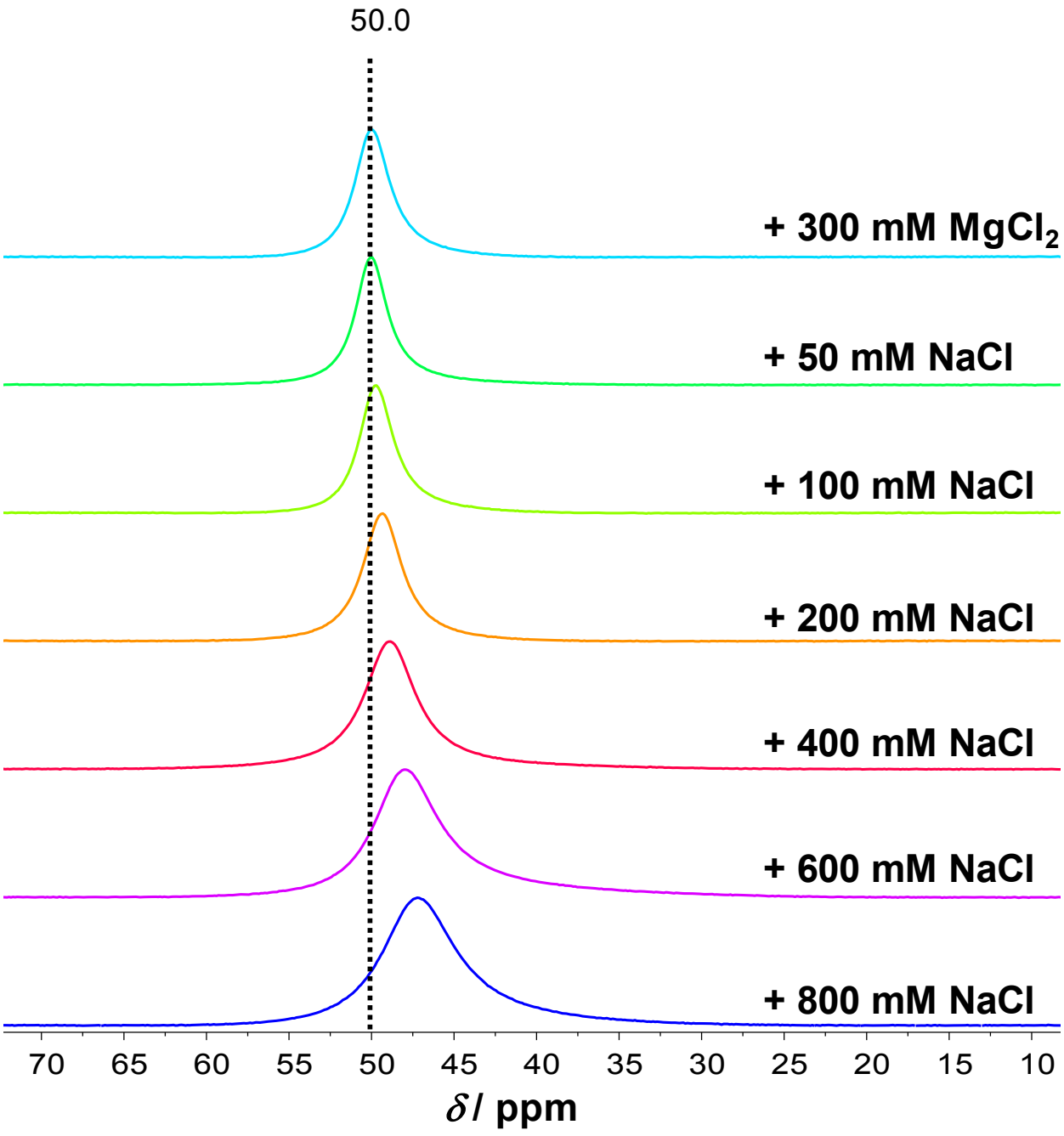

Figure S5 | ^{35}Cl NMR spectra of NaCl and $MgCl_2$ in EMIM-Ac (T = 343 K). The ^{35}Cl NMR chemical shift changes systematically and the line width increases with increasing NaCl concentration, indicating that Cl^- experiences speciation and intermediate to fast exchange at least at the higher NaCl concentrations or that the viscosity of the solution changes. Importantly, the ^{35}Cl NMR chemical shift appears to converge with decreasing NaCl concentration towards the resonance observed with 300 mM $MgCl_2$ present. This implies that Cl^- does not coordinate to Mg^{2+}. The fact that the ^{35}Cl NMR chemical shift changes with increasing NaCl concentration then may reflect interaction of Na^+ with Cl^-, and that the equilibrium is shifted towards the species involving Na^+ at higher NaCl concentration.

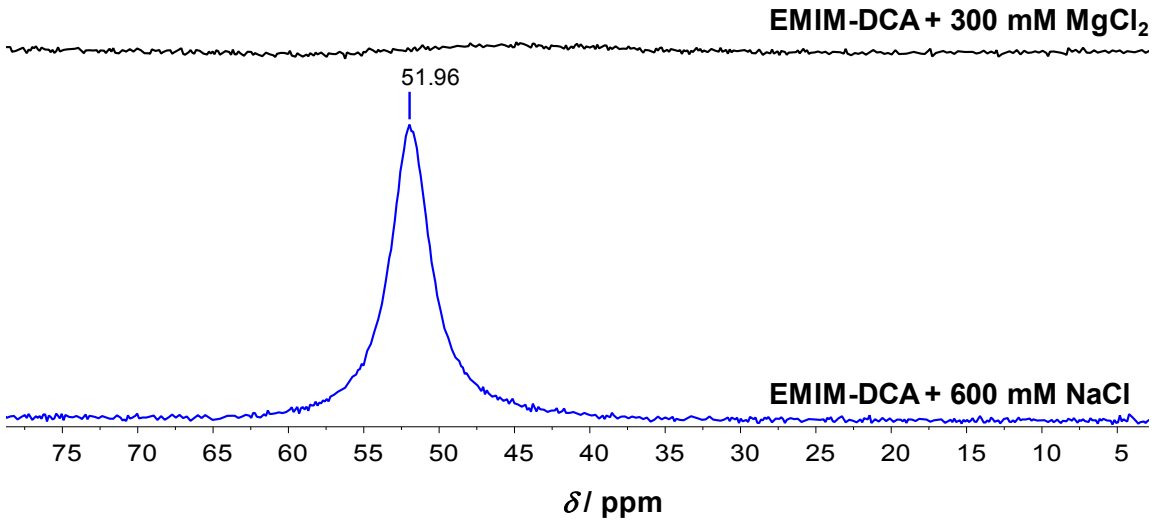

Figure S6 | ^{35}Cl NMR spectra of NaCl and $MgCl_2$ in EMIM-DCA (T = 343 K). NaCl dissolved in EMIM-DCA gives a clear ^{35}Cl resonance, while no ^{35}Cl resonance was reliably identified for $MgCl_2$ dissolved in EMIM-DCA, indicating that free Cl^- is in intermediate exchange with Cl^- coordinated to Mg^{2+}, but the number of coordinating Cl^- cannot be derived.

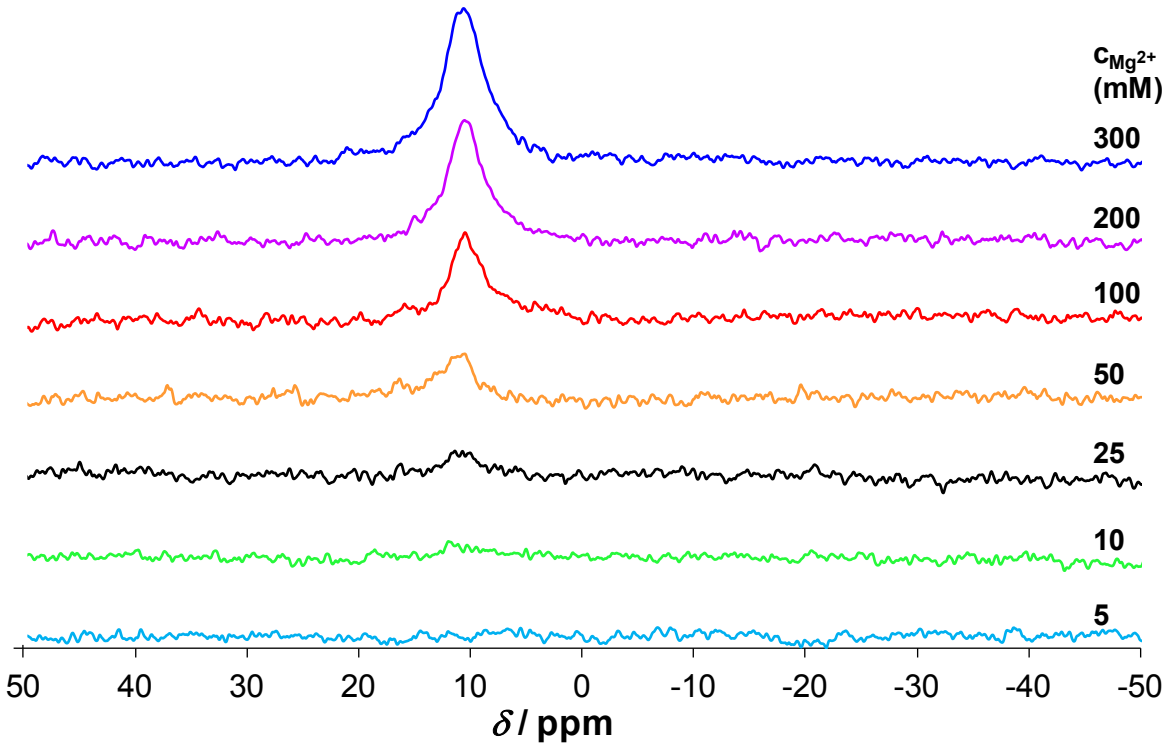

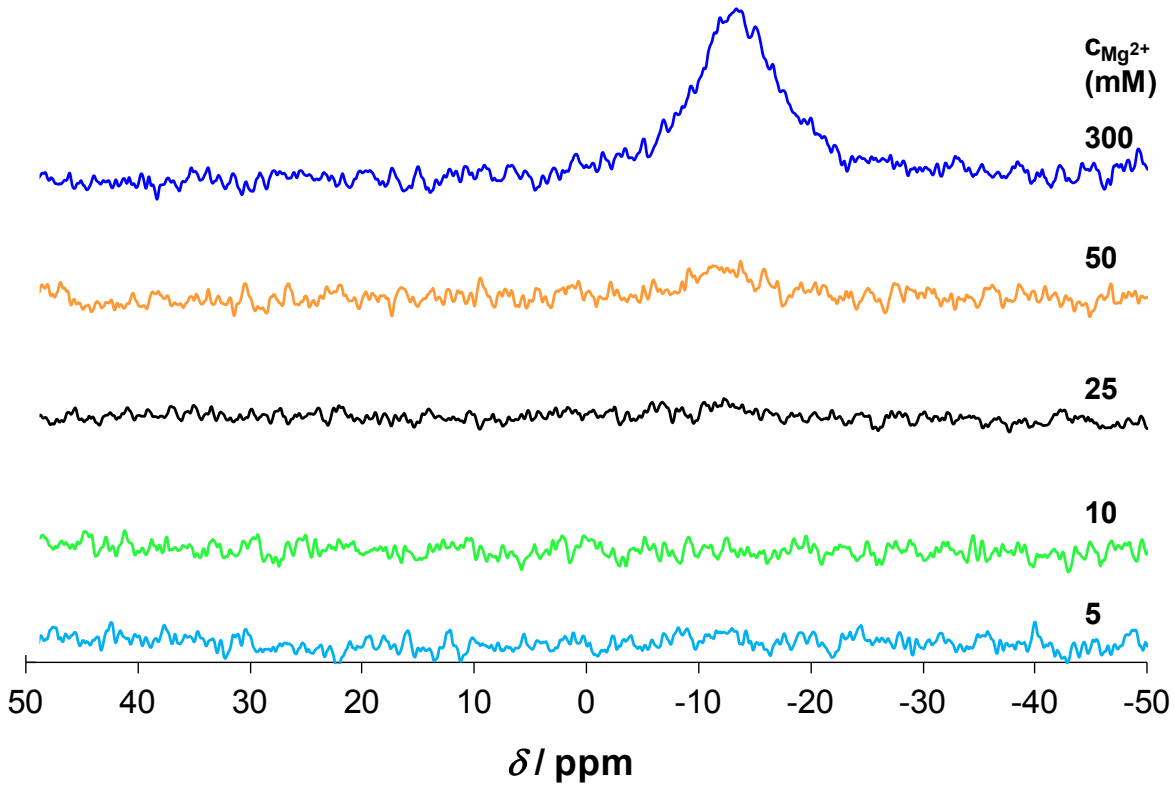

Figure S7 | Top: Concentration dependent ^{25}Mg NMR series in EMIM-Ac; Bottom: Concentration dependent ^{25}Mg NMR series in EMIM-DCA (T = 343 K).

Table S5 | ^{25}Mg NMR of $MgCl_2$ in EMIM-Ac and EMIM-DCA. All samples were prepared independently in order to estimate the chemical shift and standard deviation. The chemical shifts are reported with respect to 11 M $MgCl_2$ in H_2O. The average of the chemical shifts are 10.17 ppm ± 0.05 ppm for Mg^{2+} in EMIM-Ac and -13.26 ppm ± 0.27 ppm for Mg^{2+} in EMIM-DCA. In order to achieve a decent signal-to-noise, c_{MgCl2} was at least 100 mM in these experiments.

$MgCl_2$ in EMIM-Ac			
#	**c (mM)**	**Chemical shift (ppm)**	**FWHM (ppm)**
1	300	10.18 ± 0.01	4.19 ± 0.03
2	300	10.22 ± 0.01	4.55 ± 0.04
3	200	10.17 ± 0.01	3.66 ± 0.04
4	100	10.10 ± 0.01	3.66 ± 0.07

$MgCl_2$ in EMIM-DCA			
#	**c (mM)**	**Chemical shift (ppm)**	**FWHM (ppm)**
1	300	-13.27 ± 0.03	7.52 ± 0.08
2	300	-12.75 ± 0.03	6.65 ± 0.07
3	300	-13.20 ± 0.03	7.31 ± 0.10
4	300	-13.51 ± 0.02	7.05 ± 0.06
5	300	-13.45 ± 0.02	7.37 ± 0.06
6	300	-13.37 ± 0.03	6.98 ± 0.08

FTIR spectroscopy

Samples for FTIR spectroscopy were prepared as for NMR spectroscopy using only the pure ionic liquids or by dissolving $MgCl_2$ (anhydrous, ≥ 98 % purity, purchased from Sigma–Aldrich) in EMIM-Ac and in EMIM-DCA. All samples were placed under vacuum overnight to reduce potential water contamination. FTIR spectra were recorded on liquid films obtained by placing 5 µL solution between two CaF_2 windows of a SpectraTech FT04-036 demountable sandwich cell without the use of a spacer. A Nicolet Magna-IR 560 ESP instrument was used with a KBr beamsplitter and a DTGS detector. OMNIC software was used to obtain and average 64 scans with a resolution of 2.00 cm^{-1} and a data spacing of 0.964 cm^{-1}. To normalize the spectra, the intensity of the imidazolium C=C / C=N signal at 1590 cm^{-1} was adjusted to the same value. This also led to normalization of the C-H stretching signals around 3100 cm^{-1}. Mathematical deconvolution of the FTIR peaks corresponding to DCA vibrations in the 1800 cm^{-1} – 2500 cm^{-1} range was performed using OriginPro 2018b. For all spectra, the baseline was adjusted to zero and then three, respectively five, Lorentzian functions were fitted for pure EMIM-DCA and EMIM-DCA with $MgCl_2$ added. The small peak just above 2100 cm^{-1} could not be included in the deconvolution in a satisfactory manner.

The FTIR spectra indicate the presence of water in EMIM-Ac, while this broad IR signal at ~3300 cm^{-1} is not as pronounced in EMIM-DCA, see Figure S8. Note that 0.01 % (by volume) water in the ionic liquids corresponds to a concentration of 5.5 mM, i.e ~1 water molecule per 5 Mg^{2+} in the experiments with 25 mM Mg^{2+} (main text Figure 2). Strong IR transitions are observed at ~2131 cm^{-1} and 2230 cm^{-1} from stretching vibrations of the DCA anion in EMIM-DCA. Upon addition of Mg^{2+} to EMIM-DCA the intensity of these transitions decrease, while new signals appear at slightly higher wavenumbers, indicating binding of DCA to Mg^{2+}.

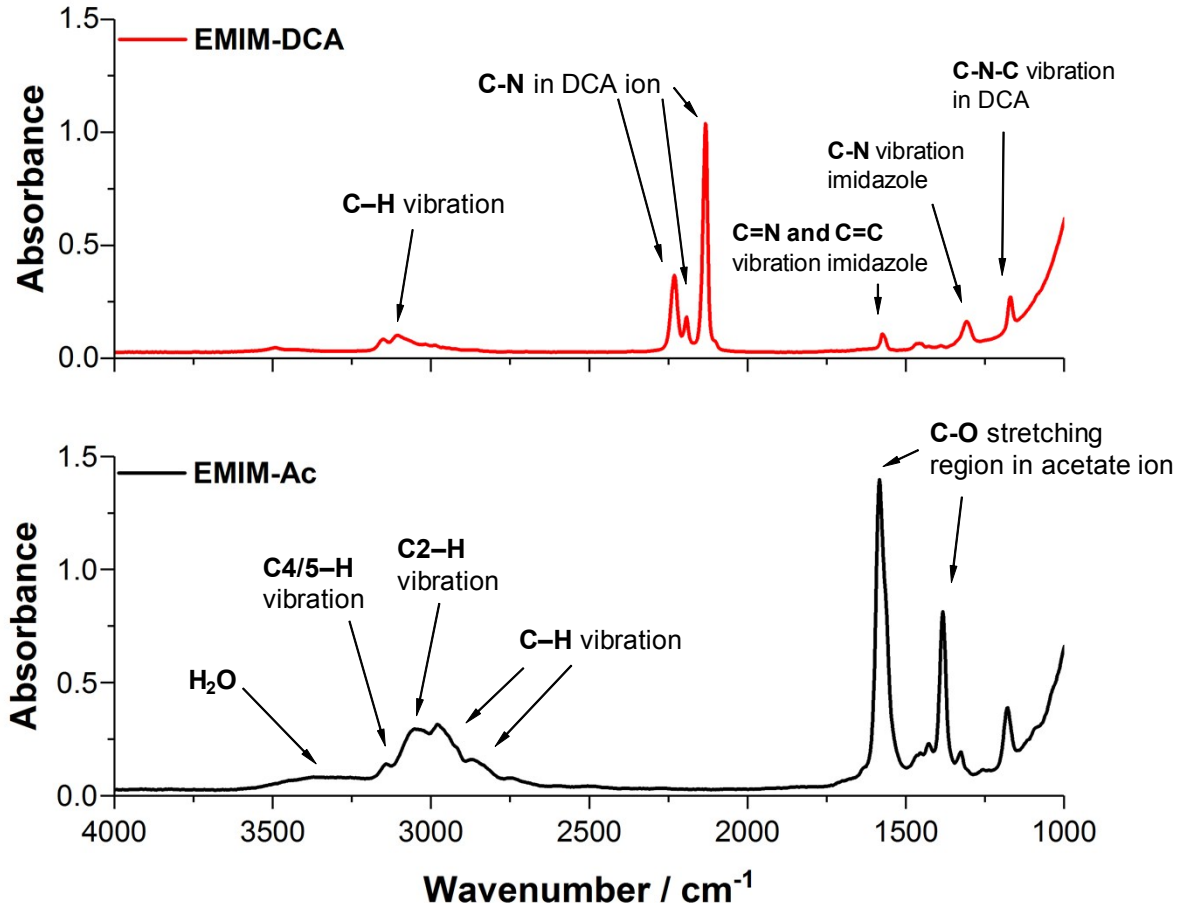

Figure S8 | FTIR spectra of pure EMIM-Ac and pure EMIM-DCA (T = 298 K), see the text for details.

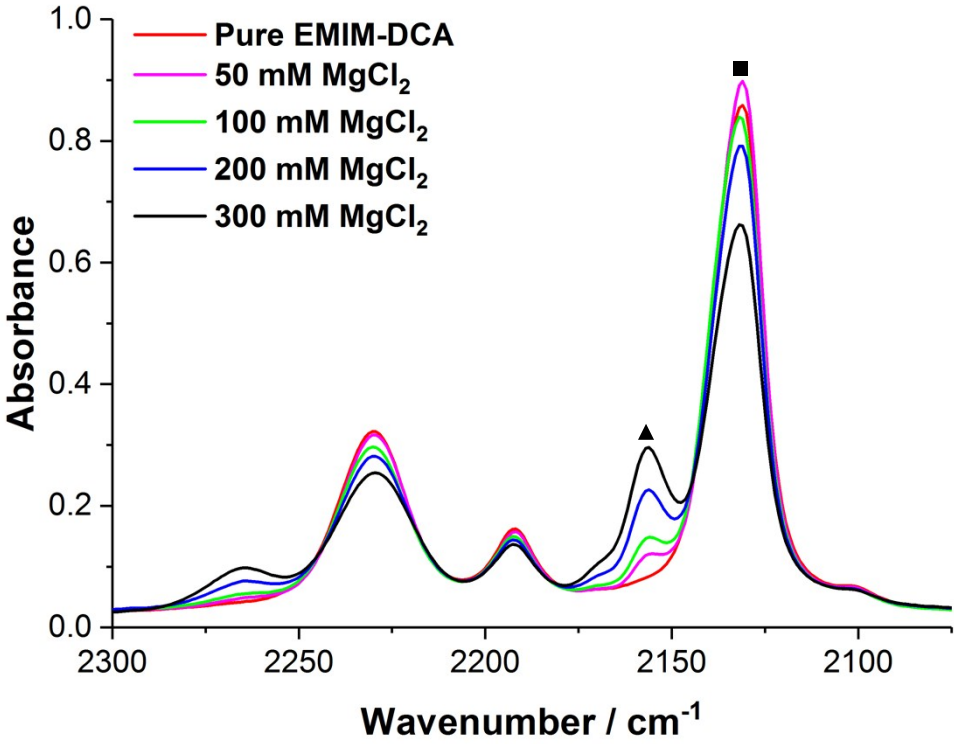

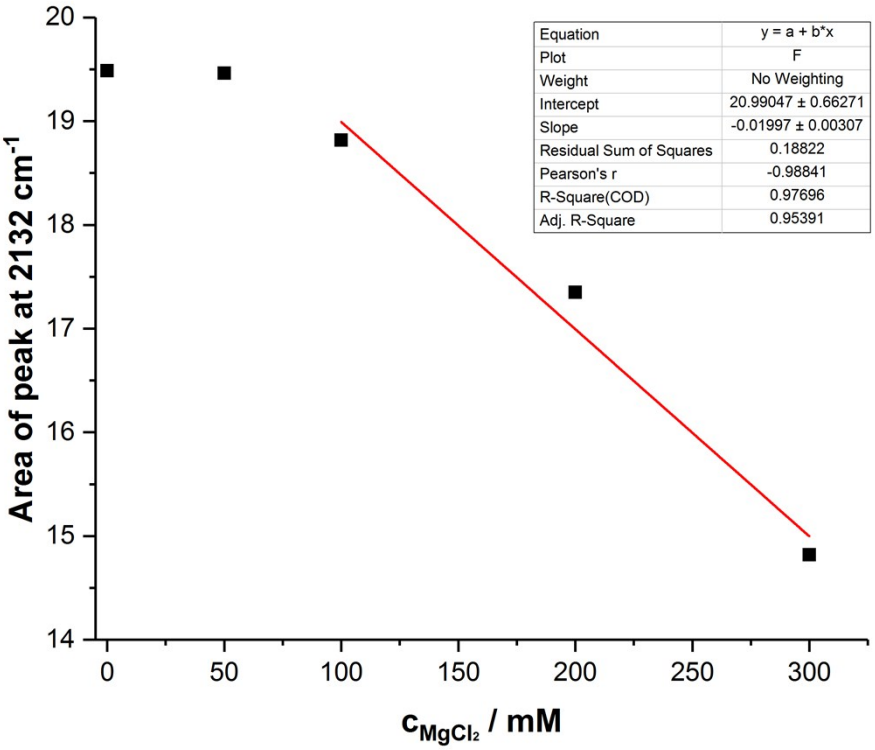

Equation	y = a + b*x
Plot	F
Weight	No Weighting
Intercept	20.99047 ± 0.66271
Slope	-0.01997 ± 0.00307
Residual Sum of Squares	0.18822
Pearson's r	-0.98841
R-Square(COD)	0.97696
Adj. R-Square	0.95391

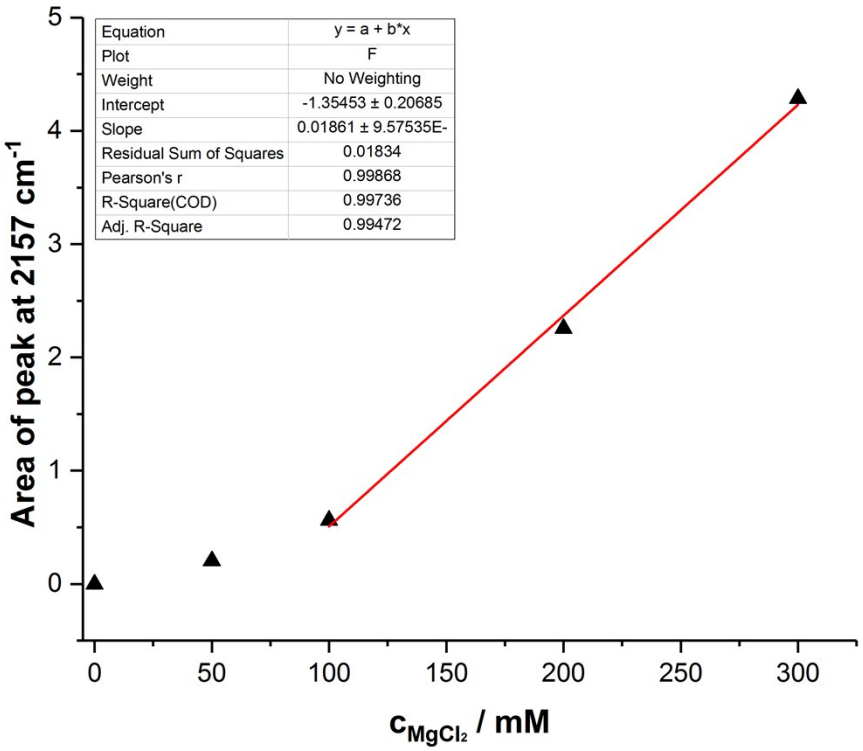

Figure S9 | FTIR spectra of EMIM-DCA + 0 – 300mM $MgCl_2$ (T = 298 K). The decrease in intensity (peak area) of the CN stretching vibration at 2132 cm^{-1} for free DCA upon addition of $MgCl_2$ may be used to estimate the DCA coordination number (CN) of Mg^{2+}, giving CN ~ 6 at concentrations above ~100 mM $MgCl_2$. The approximately linear increase of the peak area at 2157 cm^{-1} at concentrations above 100 mM indicates that $MgCl_2$ is soluble in EMIM-DCA at least up to 300 mM. These data additionally indicate that the Cl^- coordination number is small (<1) at c_{Cl^-} below 0.6 M, despite the fact that it is observable as line broadening in ^{35}Cl NMR (Figure S7). Attempts to carry out similar estimates of the number of acetate anions coordinating to Mg^{2+} in EMIM-Ac was hindered by the signals from water partly coinciding with the vibrational frequencies of acetate.

Quantum chemical calculations

All structures with trans/cis isomers were studied in the trans conformation, and for the $[Mg(DCA)_3(H_2O)_3]^-$ complex the mer-conformer was selected. The geometry of the complexes was first optimized at the B3LYP/pc-2 level[8, 9] including vibrational analysis, demonstrating in all cases that a minimum on the potential energy surface was achieved. The shielding tensors, presented as the isotropic shielding, σ, and electric field gradients (EFGs), presented as the principal component in the principal axis system, V_{zz}, and the asymmetry parameter $\eta=(V_{xx}-V_{yy})/V_{zz}$, were then calculated at the B3LYP/pcSseg-2 level[10]. Solvent effects were included in both steps of the calculations using the polarizable continuum model[11] in its integral equation formalism variant (IEF-PCM). Due to the missing parameters for the ionic liquids, a solvent, 2-heptanone, with a dielectric constant of 11.7 closest to the experimental value for EMIM-DCA, see Table S2, was chosen. There appears to be no published value for the dielectric constant for EMIM-Ac, and we assume that the same dielectric constant may be used for EMIM-Ac. This choice does not affect the conclusion in the main text. All calculations were carried out with the Gaussian 16 program[12].

β-NMR Spectroscopy

The ionic liquid samples used for β-NMR spectroscopy were prepared by dissolving $MgCl_2$ (2.4 mg; purchased from Sigma–Aldrich; ≥ 98 % purity, M=95.21g mol^{-1}) in EMIM-Ac (1-ethyl-3-methyl-imidazolium acetate 1 mL; purchased from Sigma–Aldrich; ≥ 95 % purity, *c*=6.033 M) and in EMIM-DCA (1-ethyl-3-methyl-imidazolium dicyanamide 1 mL; purchased from Sigma–Aldrich; ≥ 98 % purity, *c*=6.264M), leading to a final concentration of Mg^{2+} of 25 mM. The sample was placed under vacuum 12 h prior to the β-NMR experiment to reduce the potential water contamination. During transfer of the sample to the beam line, it was exposed to air for some minutes.

β-NMR experiments were performed at TRIUMF's ISAC-I facility in Vancouver, BC, Canada. ^{31}Mg (I = 1/2, $T_{1/2}$ = 236 ms, $\gamma/(2\pi)$ = −13.47 MHz T^{-1})[13, 14] was generated from a uranium carbide production target[15] irradiated with a 480 MeV, 10 μA proton beam. The target was coupled to a resonant laser ion source[16, 17] and a 40 keV beam of $^{31}Mg^{+}$ was extracted with an intensity of ∼10^5 ions/s. The ion beam was spin-polarized in-flight by collinear optical pumping with circularly polarized resonant laser light[18]. A longitudinal holding field of 1.3 mT along and after the polarizer section[19] of the beamline was necessary to preserve the nuclear spin-polarization of the radical ion beam during transport to a dedicated high-field spectrometer[20, 21].

The nuclear spin polarized $^{31}Mg^{+}$ ions were implanted into the ionic liquid samples housed in dimpled aluminum holders compatible with the spectrometer's cold-finger cryostat. The ion beam was focused to ∼2 mm diameter and centered on the liquid samples prior to each of the resonance measurements.

In the β-NMR measurements, the nuclear spin-polarization of $^{31}Mg^{+}$ was monitored through its anisotropic β-decay; the direction of the emitted β-rays is probabilistically correlated with the orientation of the nuclear spin at the moment of decay. The observed *asymmetry* of these β-emissions is proportional to the average longitudinal nuclear spin-polarization[22, 23]. The proportionality factor depends on the β-decay properties of the probe nucleus and the detection geometry used in the experiment. Resonance measurements were collected with a continuously implanted $^{31}Mg^{+}$ beam under an applied field B_0 = 3.41 T. A continuous-wave (CW) radio-frequency (RF) transverse magnetic field B_1 was slowly stepped through a range of frequencies near the Larmor frequency of ^{31}Mg of 46 MHz at an external field of 3.4 T. The spin of any on-resonance ^{31}Mg is rapidly precessed by B_1, destroying the average time-integrated spin-polarization, resulting in a reduction of the observed β-decay asymmetry. In these measurements, the frequency scans are repeated, with both the direction of the frequency sweep and the helicity of the polarizing laser light alternated, and these scans are then combined (*i.e.*, averaged) into helicity-resolved spectra[23]. A typical ^{31}Mg resonance is observable within only minutes, but high-resolution spectra can require up to ∼2 h. While the standard reference for ^{25}Mg NMR is typically a Mg^{2+} salt solution[24], such samples are incompatible with the ultra-high vacuum used in these experiments[21]. For ^{31}Mg, single crystal MgO with $B_0 \parallel (100)$ was used as an *ex situ* reference (FWHM ~ 42 ppm at 45.9 MHz, CRYSTAL GmbH). This choice is arbitrary, but reasonable given the relatively narrow ^{31}Mg linewidths[25,30] for solids, and consistent with the convention used in ^{8}Li β-NMR experiments[23, 26].

To analyze the β-NMR data, the helicity-resolved resonance spectra were fit to a sum of Lorentzians and a baseline, the latter of which is determined by the ^{31}Mg spin-lattice relaxation rate[27] and caps the maximum absolute intensity of the observed line. For each measurement, the spectra in both helicities were fit simultaneously using a global fitting procedure that shared the resonance frequencies and linewidths as common fit parameters. The optimum global non-linear weighted least-squares fits were found using custom C++ code leveraging the MINUIT[28] minimization routines implemented within ROOT[29].

The accuracy of the recorded β-NMR chemical shifts is affected by the stability of the external magnetic field. For this reason, the reference resonance for MgO was determined repeatedly over the ~4 days that the ^{31}Mg β-NMR experiments covered. Indeed a drift of in total ~20 ppm was observed during the initial 24 hours, and later stabilized. To extract meaningful chemical shifts for the measurements in pure EMIM-Ac which were carried within these 24 hours, and their associated uncertainties, it was necessary to interpolate between these MgO calibration measurements. For EMIM-Ac+25 mM $MgCl_2$, EMIM-DCA +25 mM $MgCl_2$, and pure EMIM-DCA, the MgO calibrations were quite constant, hence, no interpolation was necessary.

The absolute values of the chemical shifts in Figure 2 of the main text are reported with respect to different references for ^{31}Mg β-NMR (MgO single crystal) and ^{25}Mg NMR (11 M $MgCl_2$ solution). However, correcting for this (MgO exhibits a chemical shift of 26 ppm with respect to 11 M $MgCl_2$)[30] does not fully account for the difference of ~45 ppm between the ^{31}Mg β-NMR and ^{25}Mg NMR spectra, i.e. although the precision of the ^{31}Mg β-NMR chemical shifts is adequate, i.e. the relative values of chemical shifts of the ionic liquids are determined reliably within a few ppm (and even less than 1 ppm for resonances observed in the same spectrum), the accuracy appears to be about 20 ppm off. This may be due to minor differences of for example sample holders for the MgO crystal and the ionic liquids, perturbing the external magnetic field in the ^{31}Mg β-NMR experiments.

Table S6 | ^{31}Mg β-NMR data. Chemical shifts with respect to crystalline MgO have been corrected for the field drift, while frequencies in Hz are the original values from the experiment without any field drift correction. The spectra for two first entries (EMIM-DCA+25 mM $MgCl_2$ and EMIM-Ac+25 mM $MgCl_2$) are presented in the main text Figure 2, while the two last entries (for the pure ionic liquids) are presented in the main text Figure 3.

Sample	**1st resonance**	**FWHM**	**2nd resonance**	**FWHM**	**3rd resonance**	**FWHM**
EMIM-DCA + 25 mM $MgCl_2$	-60.2 ± 2.4 ppm	2.5 ± 0.1 ppm	-52.0 ± 2.4 ppm	5.9 ± 0.7 ppm	-	-
	45889759 ± 1 Hz	114 ± 4 Hz	45890138 ± 13 Hz	272 ± 32 Hz	-	-
EMIM-Ac + 25 mM $MgCl_2$	-38.1 ± 2.4 ppm	5.7 ± 1 ppm	-31.9 ± 2.4 ppm	3.4 ± 0.2 ppm	-	-
	45890772 ± 19 Hz	262 ± 66 Hz	45891057 ± 2 Hz	157 ± 8 Hz	-	-
EMIM-DCA	-61.4 ± 2.4 ppm	3.0 ± 0.2 ppm	-51.7 ± 2.4 ppm	6.2 ± 0.4 ppm	-43.2 ± 2.4 ppm	4.6 ± 0.5 ppm
	45889704 ± 3 Hz	140 ± 18 Hz	45890148 ± 5 Hz	283 ± 18 Hz	45890539 ± 8 Hz	210 ± 22 Hz
EMIM-Ac	-30.0 ± 9.1 ppm	4.2 ± 0.7 ppm	-26.9 ± 9.12 ppm	7.8 ± 0.9 ppm	-	-
	45891282 ± 10 Hz	195 ± 32 Hz	45891422 ± 34 Hz	356 ± 42	-	-

On the linewidth of the β-NMR resonances

First, it should be noted that the spectrometer/measurement was designed for broad solid state spectra, and not with the very high resolution spectroscopy of liquids in mind, in contrast to a conventional commercial NMR spectrometer which is highly refined for such measurements. Here, we include some estimates of various contributions to the observed linewidth:

1) The ^{31}Mg lifetime gives us $(1/\tau)(1/\nu_{Larmor}) \sim 0.09$ ppm (with τ being the lifetime of the radioisotope and ν_{Larmor} the Larmor frequency), so this is not a significant source of linewidth.

2) The Oxford Instruments superconducting solenoid magnet has a specification of 10 ppm homogeneity over the central cm. This homogeneity is, however, modified by the presence of the cryostat assembly. While the cryostat is constructed of materials that are as nonmagnetic as possible, we cannot exclude some additional field inhomogeneity from its magnetization. The sample and beam-spot were a small fraction of the central cm, and the same sample holder and sample volume was used in all the experiments (except for the MgO crystal reference). We estimate that these effects could give rise to a variation up to a few ppm.

3) Magnet drift during the course of a 30 minute experiment would yield a ~0.2 ppm drift in the resonance frequency and hence a broadening on this order.

4) The measurement uses a small amplitude continuous wave radiofrequency magnetic field H1. In contrast to pulsed NMR, the spectrum measured this way is "power broadened", meaning that the intrinsic spectral lineshape is convoluted with a power broadening Lorentzian of width gamma H1. For the H1 field used (0.09 Oe), this accounts for a broadening of ~2.5 ppm at the resonance field. This is a significant fraction of the observed width.

5) Finally, beyond these instrumental, technical contributions, it is possible that dynamic effects (slow tumbling and exchange dynamics) in the liquid may also contribute.

Taken together the listed contributions are of the same order of magnitude as the observed linewidths, see figures 2 and 3 in the main text.

References

1. Wilkes, J. S.; Zaworotko, M. J. *Chem Commun* 1992, **13**, 965.
2. MacFarlane, D. R.; Forsyth, S. A.; Golding, J.; Deacon, G. B. *Green Chem* 2002**, 4(5)**, 444.
3. Hunger, J.; Stoppa, A.; Schrodle, S.; Hefter, G.; Buchner, R. *Chemphyschem* 2009, **10(4)**, 723.
4. Weingärtner, H., In *Zeitschrift für Physikalische Chemie*, 2006; **220**, 1395.
5. Freire, M. G.; Teles, A. R. R.; Rocha, M. A. A.; Schroder, B.; Neves, C. M. S. S.; Carvalho, P. J.; Evtuguin, D. V.; Santos, L. M. N. B. F.; Coutinho, J. A. P. *J Chem Eng Data* 2011**, 56(12)**, 4813.
6. Korson, L.; Drost-Hansen, W.; Millero, F. J. *J Phys Chem* 1969**, 73(1)**, 34.
7. Hesse-Ertelt, S.; Heinze, T.; Kosan, B.; Schwikal, K.; Meister, F. *Macromolecular Symposia* 2010, **294(2)**, 75.
8. Jensen, F. *J Chem Phys* 2001, **115(20)**, 9113.
9. Jensen, F. *J Phys Chem A* 2007**, 111(44)**, 11198.
10. Jensen, F. *J Chem Theory Comput* 2015, **11(1)**, 132.
11. Tomasi, J.; Mennucci, B.; Cances, E. *J Mol Struc-Theochem* 1999, **464(1-3)**, 211.
12. Frisch, M. J.; Trucks, G. W.; Schlegel, H. B.; Scuseria, G. E.; Robb, M. A.; Cheeseman, J. R.; Scalmani, G.; Barone, V.; Petersson, G. A.; Nakatsuji, H.; Li, X.; Caricato, M.; Marenich, A. V.; Bloino, J.; Janesko, B. G.; Gomperts, R.; Mennucci, B.; Hratchian, H. P.; Ortiz, J. V.; Izmaylov, A. F.; Sonnenberg, J. L.; Williams; Ding, F.; Lipparini, F.; Egidi, F.; Goings, J.; Peng, B.; Petrone, A.; Henderson, T.; Ranasinghe, D.; Zakrzewski, V. G.; Gao, J.; Rega, N.; Zheng, G.; Liang, W.; Hada, M.; Ehara, M.; Toyota, K.; Fukuda, R.; Hasegawa, J.; Ishida, M.; Nakajima, T.; Honda, Y.; Kitao, O.; Nakai, H.; Vreven, T.; Throssell, K.; Montgomery Jr., J. A.; Peralta, J. E.; Ogliaro, F.; Bearpark, M. J.; Heyd, J. J.; Brothers, E. N.; Kudin, K. N.; Staroverov, V. N.; Keith, T. A.; Kobayashi, R.; Normand, J.; Raghavachari, K.; Rendell, A. P.; Burant, J. C.; Iyengar, S. S.; Tomasi, J.; Cossi, M.; Millam, J. M.; Klene, M.; Adamo, C.; Cammi, R.; Ochterski, J. W.; Martin, R. L.; Morokuma, K.; Farkas, O.; Foresman, J. B.; Fox, D. J. *Gaussian 16*, Wallingford, CT, 2016.
13. Neyens, G.; Kowalska, M.; Yordanov, D.; Blaum, K.; Himpe, P.; Lievens, P.; Mallion, S.; Neugart, R.; Vermeulen, N.; Utsuno, Y.; Otsuka, T. *Phys Rev Lett* 2005**, 94(2)**, 022501.
14. Kowalska, M.; Yordanov, D. T.; Blaum, K.; Himpe, P.; Lievens, P.; Mallion, S.; Neugart, R.; Neyens, G.; Vermeulen, N. *Physical Review C* 2008, **77(3)**, 034307.
15. Kunz, P.; Bricault, P.; Dombsky, M.; Erdmann, N.; Hanemaayer, V.; Wong, J.; Lützenkirchen, K. *J Nucl Mater* 2013**, 440(1)**, 110.
16. Lassen, J.; Li, R.; Raeder, S.; Zhao, X.; Dekker, T.; Heggen, H.; Kunz, P.; P. Levy, C. D.; Mostanmand, M.; Teigelhöfer, A.; Ames, F. *Hyperfine Interact* 2017, **238(1)**, 33.
17. Lassen, J.; Bricault, P.; Dombsky, M.; Lavoie, J. P.; Gillner, M.; Gottwald, T.; Hellbusch, F.; Teigelhöfer, A.; Voss, A.; Wendt, K. D. A. *AIP Conference Proceedings* 2009, **1104(1)**, 9.
18. Levy, C. D. P.; Pearson, M. R.; Dehn, M. H.; Karner, V. L.; Kiefl, R. F.; Lassen, J.; Li, R.; MacFarlane, W. A.; McFadden, R. M. L.; Morris, G. D.; Stachura, M.; Teigelhöfer, A.; Voss, A. *Hyperfine Interact* 2016**, 237(1)**, 162.
19. Levy, C. D. P.; Pearson, M. R.; Kiefl, R. F.; Mané, E.; Morris, G. D.; Voss, A. *Hyperfine Interact* 2014, **225(1)**, 165.
20. Morris, G. D.; MacFarlane, W. A.; Chow, K. H.; Salman, Z.; Arseneau, D. J.; Daviel, S.; Hatakeyama, A.; Kreitzman, S. R.; Levy, C. D. P.; Poutissou, R.; Heffner, R. H.; Elenewski, J. E.; Greene, L. H.; Kiefl, R. F. *Phys Rev Lett* 2004, **93(15)**, 157601.
21. Morris, G. D. *Hyperfine Interact* 2014, **225(1)**, 173.
22. Ackermann, H.; Heitjans, P.; Stöckmann, H.-J. In *Hyperfine Interactions of Radioactive Nuclei*; Christiansen, J., Ed.; Springer Berlin Heidelberg: Berlin, Heidelberg, 1983; pp 291-361.
23. MacFarlane, W. A. *Solid State Nucl Mag* 2015, **68-69**, 1.
24. Annual reports on NMR spectroscopy. In Academic Press: London ; New York, 1970; p volumes.
25. Stachura, M.; McFadden, R. M. L.; Chatzichristos, A.; Dehn, M. H.; Gottberg, A.; Hemmingsen, L.; Jancso, A.; Karner, V. L.; Kiefl, R. F.; Larsen, F. H.; Lassen, J.; Levy, C. D. P.; Li, R.; MacFarlane, W. A.; Morris, G. D.; Pallada, S.; Pearson, M. R.; Szunyogh, D.; Thulstrup, P. W.; Voss, A. *Hyperfine Interact* 2017, **238**, 38.
26. MacFarlane, W. A.; Parolin, T. J.; Cortie, D. L.; Chow, K. H.; Hossain, M. D.; Kiefl, R. F.; Levy, C. D. P.; McFadden, R. M. L.; Morris, G. D.; Pearson, M. R.; Saadaoui, H.; Salman, Z.; Song, Q.; Wang, D. *Journal of Physics: Conference Series* 2014, **551(1)**, 012033.
27. Hossain, M. D.; Saadaoui, H.; Parolin, T. J.; Song, Q.; Wang, D.; Smadella, M.; Chow, K. H.; Egilmez, M.; Fan, I.; Kiefl, R. F.; Kreitzman, S. R.; Levy, C. D. P.; Morris, G. D.; Pearson, M. R.; Salman, Z.; MacFarlane, W. A. *Physica B* 2009**, 404(5-7)**, 914.
28. James, F.; Roos, M. *Comput Phys Commun* 1975, **10(6)**, 343.
29. Brun, R.; Rademakers, F. *Nuclear Instruments and Methods in Physics Research Section A: Accelerators, Spectrometers, Detectors and Associated Equipment* 1997**, 389(1)**, 81.
30 McFadden, R. M. L.; Chatzichristos A.; Dehn, M.; Fujimoto, D.; Funakubo, H.; Gottberg, A.; Hitosugi, T.; Karner, V.; Kiefl, R.; Kurokawa, M.; Lassen, J.; Levy, C.D.P.; Li, R.; Morris, G.; Pearson, M.; Shiraki, S.; StachuraM, M.; Sugiyama, J.; Szunyogh, D.; MacFarlane, A. *JPS Conf. Proc.* 2018, **21**, 011047.